Title: Mapping the agricultural drought based on the long-term AVHRR NDVI and North American Regional Reanalysis (NARR) in the United States, 1981-2013

Author:
Junyu Lu, Ph.D. (Corresponding author)
Department of Geography
University of South Carolina
709 Bull Street, Columbia, SC 29208, United States
Tel: (224)999-2218, Email address: jlu@email.sc.edu

Gregory J. Carbone, Ph.D.
Professor, Department of Geography
University of South Carolina
709 Bull Street, Columbia, SC 29208, United States
Tel: (803)777-0682, Email address: carbone@mailbox.sc.edu

Peng Gao, Ph.D.
Department of Geography
University of South Carolina
709 Bull Street, Columbia, SC 29208, United States
Tel: (803)931-6309, Email address: gaop@email.sc.edu

Acknowledgement:
This work was supported by the National Oceanic and Atmospheric Administration (NOAA) Climate Program Office (grant no. NA11OAR4310148 and NA16OAR4310163) to the Carolinas Integrated Sciences and Assessments.

Mapping the agricultural drought based on the long-term AVHRR NDVI and North American Regional Reanalysis (NARR) in the United States, 1981-2013

Abstract: To provide a long-term perspective of drought variability from 1981 to present, we develop a new monthly agriculturally-based drought index called the Integrated Scaled Drought Index (ISDI). This index integrates Normalized Difference Vegetation Index (NDVI) from Advanced Very High Resolution Radiometer (AVHRR) data (available from 1981 to present), land surface temperature (LST), precipitation (PCP), and soil moisture (SM) data from North American Regional Reanalysis (NARR) project (available from 1979 to present). This new agriculturally-based drought index incorporates important components controlling agricultural drought, particularly soil moisture, for which there are limited in-situ observations through time and across space. The optimum weights for each component of the ISDI are determined by correlation analysis with commonly used in-situ drought indices, such as the Palmer Drought Severity Index (PDSI), the Palmer Modified Drought Index (PMDI), the Palmer's Z-index, and the Standardized Precipitation Index (SPI) at different time scales. Resulting ISDI maps are also visually compared with United States Drought Monitor (USDM) and Vegetation Drought Response Index (VegDRI) maps for empirical validation. ISDI shows strong agreement with these two national-wide drought monitoring systems. ISDI also shows strong linear correlations with corn yield anomalies in July and with soybean yield anomalies in August and strong spatial correspondence with county-level corn/soybean yield anomalies during major drought events. These results illustrate the robustness and usefulness of ISDI. This agriculturally-based drought index integrates the benefits of numerical model simulation and remote sensing technology to

account for interannual variability of drought for the longest possible time-frame in the satellite era. This long-term monthly drought index provides a longer historical perspective of drought impacts since 1981. It can be generalized to incorporate other satellite data or in-situ observation and has the potential for operational drought monitoring and assessment.

Keywords: Agricultural drought; Drought indices; Soil moisture; AVHRR NDVI; Crop yield anomalies

1. Introduction

Drought is a devastating, recurring, and widespread natural hazard with complicated socioeconomic, environmental, and ecological impacts (AMS, 1997). Drought is a costly hazard in the United States historically, in which Consumer Price Index (CPI) adjusted drought losses exceeded 223.8 billion dollars from 1980-2016, roughly accounting for 20% of all losses from major weather events (NOAA, 2018). Within the agricultural sector, drought affects soil moisture availability and contributes to crop failures and pasture decline, posing risks on food security.

Drought impacts depend on the timing, severity, and duration of the events, and on resilience. Drought monitoring and early warning are critical for agricultural production and risk adaptation as effective drought quantification can mitigate losses. Of course, identifying and quantifying drought events is difficult due to its complex and diverse nature, reflected in its many definitions (e.g., meteorological, agricultural, hydrological, and socioeconomic), and the varying criteria used to estimate its severity (AMS, 1997; Heim, 2002; IPCC, 2001). Appropriate quantification of drought for a variety of applications (e.g., agricultural drought or hydrological drought) requires consideration of a wide range of contributing processes (Sheffield, Goteti, Wen, & Wood, 2004; Wilhite, 2000).

Drought monitoring mainly has been based on in-situ drought indices calculated from station-based, or areally-based meteorological data. The Palmer Drought Severity Index (PDSI) is based on the supply-and-demand concept of water balance equation using precipitation, temperature, and available water capacity of the soil (Palmer, 1965). The PDSI and its variations, such as the Palmer Z index (Palmer, 1965), Palmer Hydrologic Drought Index (PHDI) (Palmer, 1965), and Palmer Modified Drought Index (PMDI) (Heddinghaus & Sabol, 1991) have been widely used for drought assessment and water resources management decisions. Shafer and Dezman (1982) developed the Surface Water Supply Index (SWSI) to monitor abnormalities in surface water supply using historical records of streamflow, snow pack, precipitation, and reservoir components. The Standardized Precipitation Index (SPI) was developed to quantify precipitation deficit for different time scales based on only precipitation data (McKee, Doesken, & Kleist, 1993). Compared with PDSI, SPI requires less data, has flexible time scales, and is spatially invariant (Guttman, 1998). Recently, Vicente-Serrano, Beguería, and López-Moreno (2010) proposed the Standardized Precipitation Evapotranspiration Index (SPEI) based on precipitation and temperature data, which incorporates an evapotranspiration component into the calculation of SPI and is appropriate for detecting drought changes in the context of global warming (Vicente-Serrano et al., 2010).

Satellite remote sensing data have also been used to quantify drought when in-situ weather station observations are not available (Kogan, 1995a; Rhee, Im, & Carbone, 2010), resulting in several remote-sensing-based drought indices. Among them, the Normalized Difference Vegetation Index (NDVI) developed by Rouse, Haas, Schell, and Deering (1974) has been widely for drought monitoring (Peters et al., 2002). NDVI is the normalized reflectance difference between the near-infrared (NIR) band and visible red band since the chlorophyll A and B within vegetation leaf have peak absorption within the visible (red) portion of the electromagnetic spectrum and spongy mesophyll cells have an optimum reflection region in NIR wavelengths. NDVI can effectively reflect the physiologically functioning surface greenness level and higher NDVI values represent greater photosynthetic capacity of the vegetation canopy (Tucker, 1979). However, NDVI contains both weather-related and ecosystem components (Kogan, 1995a). Kogan (1995a) developed the Vegetation Condition Index (VCI) by linearly scaling NDVI values from 0 to 1 for each grid cell to separate weather-related components from ecosystem components. To distinguish drought effects from other environmental factors (e.g., excessive wetness, pest, plant disease), related climate information from satellite observation or in-situ observation could be integrated with NDVI data (Kogan, 1995b). In addition to VCI, thermal band based Temperature Condition Index (TCI) was developed to provide additional information on land surface temperature to distinguish vegetation stress caused by drought events from other factors (Kogan, 1995b). The linear combination of VCI and TCI results in a Vegetation Health Index (VHI), reflecting both temperature and precipitation conditions (Kogan, 1995b).

With the development of hyperspectral remote sensing, such as the Moderate Resolution Imaging Spectroradiometer (MODIS), additional remote-sensing-based drought indices have been developed. For example, B. Gao (1996) proposed the Normalized Difference Water Index (NDWI) to detect moisture status of vegetation canopy based on the Near Infrared (NIR) channel providing information on vigor of vegetation via high optimum reflection by spongy Mesophyll cells and the Shortwave Infrared (SWIR) channel providing information on changes of water content. Based on NDVI and NDWI, Gu, Brown, Verdin, and Wardlow (2007) proposed Normalized Difference Drought Index (NDDI) and demonstrated a quicker and stronger response to summer drought compared with NDVI and NDWI. Wang and Qu (2007) developed the Normalized Multi-band Drought Index (NMDI) based on the sensitivity findings that the two MODIS SWIR bands respond differently to soil moisture and vegetation moisture variations. NMDI uses NIR band centered at 860 nm channel (band 2) as the reference and uses the two water absorption SWIR channels centered at 1640 nm (band 6) and 2130 nm (band 7) as the soil moisture and vegetation moisture sensitive band respectively (Wang & Qu, 2007). NMDI provided solutions to separate vegetation moisture from soil moisture by amplifying one signal and minimizing the other (Wang & Qu, 2007).

More recently, Rhee et al. (2010) proposed the Scaled Drought Condition Index (SDCI) for monitoring agricultural drought in both arid and humid regions. This index combines three standardized scaled remote sensing variables together – the Normalized Difference Vegetation Index (NDVI), the land surface temperature (LST) from MODIS sensors, and precipitation from the Tropical Rainfall Measuring Mission (TRMM) satellite. Through validations against in-situ drought indices and United States Drought Monitor (USDM) maps, Rhee et al. (2010) demonstrated that SDCI performed better than NDVI, NMDI, NDDI, and VHI in both arid and humid regions. The formulas of several remote sensing drought indices are shown in Table 1.

Table 1 Formulas of remote sensing drought indices

Drought Indices	Formula
NDVI (Normalized Difference Vegetation Index）	$(\rho_{NIR} - \rho_{RED}) / (\rho_{NIR} + \rho_{RED})$
VCI (Vegetation Condition Index)	$(NDVI - NDVI_{min}) / (NDVI_{max} - NDVI_{min})$

TCI (Temperature Condition Index)	$(T_{max} - LST) / (LST_{max} – LST_{min})$
VHI (Vegetation Health Index)	α * VCI + β * TCI
NDWI (Normalized Difference Water Index)	$(\rho_{NIR} – \rho_{SWIR}) / (\rho_{NIR} + \rho_{SWIR})$
NDDI (Normalized Difference Drought Index)	(NDVI – NDWI) / (NDVI + NDWI)
NMDI (Normalized Multi-band Drought Index)	$(\rho_{NIR} – (\rho_{1640nm} – \rho_{2130nm})) / (\rho_{NIR} + (\rho_{1640nm} – \rho_{2130nm}))$
SDCI (Scaled Drought Condition Index)	(1/4) * scaled LST + (2/4) * scaled TRMM + (1/4) * scaled NDVI

Where ρ represents spectral reflectance; α and β represent the weights.

Vegetation indices naturally lend themselves to agricultural drought measurement, but could be enhanced with information from other variables, such as precipitation, evapotranspiration, temperature, and soil moisture (AMS, 2013). Soil moisture decline is a very important indicator of agricultural drought as it reflects antecedent precipitation, evapotranspirative losses, and determines available water supply for healthy plant growth (AMS, 1997; Keyantash & Dracup, 2002; WMO, 1975). Yet, soil moisture is one of the least observed variables in the US and elsewhere globally (Sheffield et al., 2004). Without a comprehensive, large-scale, and long-term network of in-situ soil moisture measurement (Keyantash & Dracup, 2002) and shallow observation depths of remote sensing based soil moisture conditions (Leeper, Bell, Vines, & Palecki, 2016), the use of simulated soil moisture from numerical models provides a viable alternative (Sheffield et al., 2004). Numerical models can compute the soil moisture by simulating the water balance of the soil column using precipitation, air temperature, soil temperature, soil porosity, and infiltration as inputs (Keyantash & Dracup, 2002). The commonly used and high-resolution reanalysis dataset, North American Regional Reanalysis (NARR) simulates soil moisture and serves as a good source of information for long-term soil moisture conditions. Leeper et al. (2016) demonstrated that soil moisture data from NARR could capture the timing, intensity, and spatial extent of 2012 drought using standardized soil moisture anomalies, when compared against in-situ soil moisture observations from the United States Climate Reference Network (USCRN). In the United States, there are several nation-wide drought monitoring systems, such as the United States Drought Monitor (USDM), and related indices (e.g., Vegetation Drought Response Index (VegDRI) and the Evaporative Stress Index (ESI)). These drought monitoring systems have provided national wide drought measurements since 2000.

To cover the longest time-frame during the satellite era, to learn more about year-to-year variability in growing conditions and the consequent impacts on agriculture, and to incorporate one of the most important variables in agricultural drought modeling, we develop a new monthly agriculturally-based drought index that integrates satellite-based observations of vegetation state and climate information from reanalysis dataset. We use the NDVI from NOAA's Advanced Very High Resolution Radiometer (AVHRR) sensor to take advantage of this longest NDVI time series from 1981 to present and its large area coverage. We combine this with land surface temperature (LST), precipitation (PCP), and soil moisture (SM) data from the NCEP NARR project (available 1979 to present), producing a sound, consistently blended, agriculturally-based drought index that accounts for interannual variability for the longest possible time-frame during the satellite era. Such an index can not only provide insights for historical drought impacts assessment, but also be generalized to incorporate other satellite data or in-situ observation. In addition to putting past droughts in historical context, our new index can be applied to current or future agricultural drought monitoring.

2. Data

2.1. North American Regional Reanalysis (NARR) data

Precipitation, land surface temperature, and total soil moisture content data were extracted from NARR data (Mesinger et al., 2006). The NARR data are updated monthly by NOAA's National Centers for Environmental Prediction (NCEP) and the NARR data can be accessed from the National Center for Atmospheric Research (NCAR) Research Data Archive (RDA) (https://rda.ucar.edu/datasets/ds608.0/). NARR is a regional reanalysis for North America, that contains temperatures, precipitation, wind, soil moisture, radiation, evaporation, etc. (Mesinger et al., 2006). This dataset provides a long-term climatology spanning from 1979 to present over North America at a spatial resolution of 32 km and temporal resolution of 3 hours. NARR uses a recently operational version of the NCEP regional Eta model and the Noah land-surface model and assimilates high-quality observational data, including radiosondes, hourly precipitation (with PRISM correction), surface observations, aircraft, geostationary satellites, etc. (Mesinger et al., 2006). This dataset is superior to NCEP/NCAR Global Reanalysis (GR), especially due to an advance in modeling and additional assimilation of precipitation and radiance (Mesinger et al., 2006). NARR has the potential to represent extreme events, such as floods, droughts, and their driving mechanisms (Mesinger et al., 2006).

NARR has been used widely to understand weather and climate variability across North America. Ruiz-Barradas and Nigam (2006) used NARR data to investigate the hydroclimate variability over the Great Plains. Mo and Chelliah (2006) used NARR products to produce PMDI to monitor drought in the US. Karnauskas, Ruiz-Barradas, Nigam, and Busalacchi (2008) used NARR and 40-yr European Centre for Medium-Range Weather Forecasts (ECMWF) Re-Analysis (ERA-40) data to construct a PDSI dataset. Vivoni, Tai, and Gochis (2009) used NARR to investigate the mechanisms and effects of initial soil moisture on precipitation, streamflow, and evapotranspiration during the monsoon in New Mexico. Becker, Berbery, and Higgins (2009) used NARR to examine the seasonal characteristics of precipitation and related physical mechanisms over the US. Choi, Kim, Rasmussen, and Moore (2009) used the NARR temperature and precipitation data for hydrological modeling with Semi-distributed Land Use-based Runoff Processes (SLURP). P. Gao, Carbone, and Guo (2016) used NARR data to assess and evaluate the performance of North American Regional Climate Change Assessment Program (NARCCAP) in simulating the precipitation extremes in the US.

2.2. Remote sensing data

NDVI data were obtained from the Global Inventory Monitoring and Modeling System (GIMMS) project to represent the vigor, robustness, and photosynthetic capacity of vegetation. The GIMMS project carefully assembles NDVI data from different AVHRR sensors and accounts for different deleterious effects, such as calibration losses, orbital drift, and volcanic eruptions (Pinzon & Tucker, 2014). The third generation GIMMS NDVI from AVHRR sensors is bimonthly spanning from the period from July 1981 to December 2013 with a spatial resolution of 1/12° lat/lon across the globe (Pinzon & Tucker, 2014). The GIMMS NDVI dataset was downloaded from the Ecological Forecasting Lab at NASA Ames Research Center (https://ecocast.arc.nasa.gov/data/pub/gimms/3g.v1/). The bimonthly NDVI was aggregated into monthly.

2.3. Land use/cover data

The National Land Cover Database (NLCD) products with 30m spatial resolution were used to extract the land areas of Grassland/Herbaceous (class 71), Pasture/Hay (class 81), and Cultivated Crops (class 82). We used the NLCD 2001 (Homer et al., 2007) database because this baseline is in the middle of our study period. Wickham, Stehman, Fry, Smith, and Homer (2010) used a sampling approach to assess the accuracy of NLCD 2001 and reported that the overall thematic accuracy of Anderson Level II and Level I were 78.7% and 85.3% respectively. Wickham et al. (2017) reported that the single-date overall accuracies of NLCD 2011, 2006, and 2001 were close: respectively 82%, 83%, and 83% at Level II and 88%, 89%, and 89% at Level I. The purpose of NLCD here is to extract the values of the new drought index covering those three land use types, which are used for validation of the new drought index via correlation analysis with the crop yield anomalies in section 4.3.

2.4. In-situ drought index

We obtained in-situ monthly drought indices, including the PDSI, PMDI, Palmer Z index, 1-month SPI, 2-month SPI, 3-month SPI, 6-month SPI, 9-month SPI, and 12-month SPI from 1895 to present from NOAA’s National Centers for Environmental Information (NCEI) (ftp://ftp.ncdc.noaa.gov/). These indices at the climate divisional spatial scale were primarily used for derivation and validation of the potential new drought index.

2.5. Agriculture statistics

We obtain the state-level and county-level corn and soybean yield data from 1981 to 2013 from USDA’s NASS Quick Stats tools (USDA, 2017). The crop data used here do not differentiate irrigated yield and non-irrigated yield. We used corn and soybean yield to validate and test the potential use of the new index.

3. Methods

3.1. Scaled drought indices

Monthly precipitation (PCP), soil moisture (SM), NDVI, and land surface temperature (LST) were scaled according to their historical minimum and maximum values in each pixel following Kogan (1995a) and Kogan (1995b) (Table 2). Scaling NDVI can separate climate variability from ecosystem components (Kogan, 1995b). Scaling climate variables can discriminate the weather and climate variability from spatial heterogeneity. For each pixel, the scaling process was also performed for each month since the climate conditions and vegetation states are not homogenous across months. For each pixel, the historical maximum NDVI, precipitation, and soil moisture values are scaled to 1 to indicate the wettest case; the historical minimum NDVI, precipitation, and soil moisture are scaled to 0 to indicate the driest case. The LST was used to provide additional information for vegetation stress and to determine temperature-related vegetation stress (Kogan, 1995b). Contrary to other variables, in the warm season, high temperature indicates mostly unfavorable or drought conditions, while low temperature indicates mostly favorable conditions (Kogan, 1995b). Thus, the maximum LST is scaled to 0 and the minimum LST is scaled to 1. The scaling method can make those variables representing drought conditions comparable across space and time that higher scaled values indicate relative wetter conditions and lower scaled values indicate drier conditions. These four monthly variables (PCP, SM, NDVI, and LST) are linearly combined using different weights to form a new agriculturally-based drought index: Integrated Scaled Drought Index (ISDI). The calculation of ISDI are based on all grid cells across the US.

Table 2 Formulas of scaled drought indices

Drought Indices	Formula

Scaled NDVI (VCI)	$(NDVI - NDVI_{min}) / (NDVI_{max} - NDVI_{min})$
Scaled LST	$(LST_{max} - LST) / (LST_{max} - LST_{min})$
Scaled PCP	$(PCP - PCP_{min}) / (PCP_{max} - PCP_{min})$
Scaled SM	$(SM - SM_{min}) / (SM_{max} - SM_{min})$
ISDI	α * Scaled NDVI + β * Scaled LST + γ * Scaled PCP + λ * Scaled SM

Where NDVI represents Normalized Difference Vegetation Index from GIMMS AVHRR NDVI dataset; LST, PCP, and SM represent land surface temperature, precipitation, and soil moisture from NARR dataset; α, β, γ, and λ represent the weights of single scaled variable to form the Integrated Scaled Drought Index (ISDI) and $\alpha + \beta + \gamma + \lambda = 1$; $NDVI_{min}$, LST_{min}, PCP_{min}, and SM_{min} indicate the minimum values of NDVI, land surface temperature, precipitation, and soil moisture for each pixel and each month; $NDVI_{max}$, LST_{max}, PCP_{max}, and SM_{max} indicate the maximum values of NDVI, land surface temperature, precipitation, and soil moisture for each pixel and each month.

NARR data are in GRIB format on a Lambert-conformal grid. Climate variables from NARR were resampled using piecewise linear interpolation to the spatial resolution of 1/12° lat/lon as GIMMS NDVI. NARR data and AVHRR NDVI data were all projected to UTM Zone 14N.

3.2. Correlation analysis with in-situ drought indices

We systematically created fifteen different sets of weights for four variables (PCP, SM, NDVI, and LST). We determined optimum weights by performing correlation analysis between ISDI of different weights and multiple in-situ drought indices – Palmer Z-index, PDSI, PMDI, 1-month SPI, 2-month SPI, 3-month SPI, 6-month SPI, 9-month SPI and 12-month SPI – at the climate divisional scale. NARR data and AVHRR NDVI data were spatially averaged over 344 climate divisions to facilitate correlation analysis between in-situ drought indices and ISDI of different weights. Two coastal climate divisions (0807: Keys in Florida and 2803: Coastal in New Jersey) do not have soil moisture information from NARR data and are excluded from the testing and validation process. In order to be comparable and consistent across space and time, the whole CONUS, from 1981 to present, share the same optimum weight.

3.3. Correlation analysis with crop yield data

Drought can have significant impacts on agriculture and crop yield variabilities are highly correlated with drought severity (Mishra & Cherkauer, 2010; Quiring & Papakryiakou, 2003; Trnka et al., 2007). Here, we used corn and soybean yield, to quantitatively validate the potential use of ISDI. State-level corn and soybean yield time series are detrended by locally weighted regression model (LOWESS) to remove the nonlinear and non-stationary increasing trend caused by technological advances (Lu, Carbone, & Gao, 2017). This detrending approach allows us to successfully separate out environmental and weather factors from other technological factors (Lu et al., 2017). Crop yield anomalies derived from this approach indicate the percentage of crop yield lower or higher than normal (Lu et al., 2017). We performed correlation analyses between corn/soybean yield anomalies and monthly ISDI during growing seasons (March through October) at the state level to evaluate the performance of the new drought index. Corn has five major phonological stages: emerged, silking, dough, dent, and mature and soybean has four major phonological stages: emerged, blooming, setting pods, and dropping leaves (USDA, 2009). Yield sensitivity to drought varies with stage. ISDI values were extracted from pixels of land cover types: grassland/herbaceous, pasture/hay, and cultivated crops, from NLCD 2001 and were then spatially averaged for each state.

3.4 Empirical validation with maps of USDM, VegDRI, and Gridded SPI from PRISM

ISDI with optimum weights were visually compared with United States Drought Monitor (USDM) maps and Vegetation Response Index (VegDRI) maps for empirical validation and assessment. The archives of USDM maps from 2000 to present are available from the National

Drought Mitigation Center (http://droughtmonitor.unl.edu/). The USDM map is based on climate indices, numerical models, and the inputs of regional and local experts, which is not a strictly quantitative product, but a blend of science and subjectivity (Svoboda et al., 2002). The archives of VegDRI maps from 2009 to present are also available from the National Drought Mitigation Center (http://vegdri.unl.edu/). VegDRI integrates traditional drought indicators (e.g., PDSI and SPI) and NDVI with other biophysical information to monitor vegetation responses to drought conditions using a data mining technique (Brown, Wardlow, Tadesse, Hayes, & Reed, 2008). Since the USDM and VegDRI maps are created weekly, we used the end of month maps for comparison. Further, ISDI maps were also visually compared with gridded monthly SPI3 maps for empirical validation. We calculated SPI values across CONUS using 4-km gridded PRISM (Parameter-elevation Relationships on Independent Slopes Model) precipitation dataset (Daly et al., 2008) from 1895 to 2014 as an in-situ reference of spatial variability of drought severity. We computed SPI values following the method of McKee et al. (1993), modeling precipitation accumulations of different time scales with a gamma distribution. The flow chart of research method is shown in Figure 1.

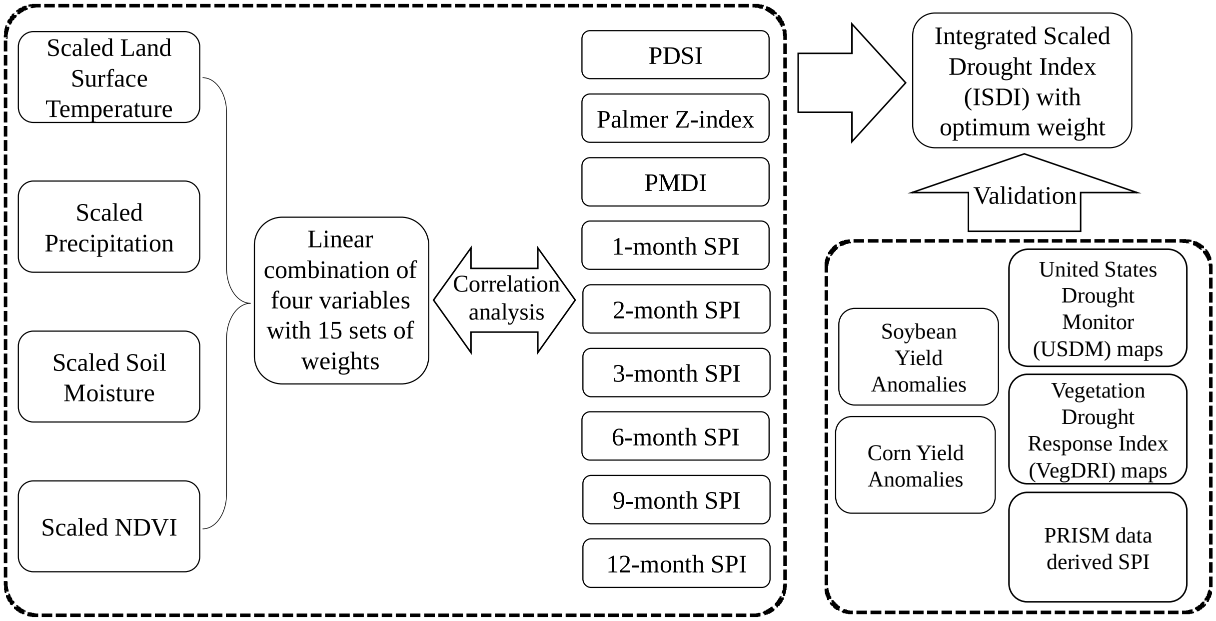

Fig. 1 Flow chart of research methods

4. Results and discussion

4.1. Correlation with in-situ drought indices

Table 3 Averaged correlation coefficients between in-situ drought indices and scaled LST, scaled PCP, scaled SM, and scaled NDVI over 342 climate divisions. The highest averaged correlation coefficient for each in-situ drought index (each column) is shown in bold.

	Correlation coefficients								
	Z-index	PDSI	PMDI	SPI1	SPI2	SPI3	SPI6	SPI9	SPI12
Scaled NDVI	0.011	0.105	0.118	-0.027	0.068	0.103	0.104	0.132	0.141
Scaled LST	0.373	0.382	0.388	0.217	0.278	0.298	0.306	0.272	0.252
Scaled PCP	**0.850**	0.468	0.446	**0.899**	**0.675**	**0.570**	0.404	0.329	0.291
Scaled SM	0.372	**0.650**	**0.704**	0.256	0.436	0.515	**0.629**	**0.664**	**0.646**

Table 3 shows the averaged correlation coefficients between in-situ drought indices and scaled LST, scaled PCP, scaled SM, and scaled NDVI for 342 climate divisions.

Scaled PCP shows higher correlation with the Palmer Z-index and shorter-duration SPI values (i.e., 1-month, 2-month, and 3-month) than with other scaled drought indices. Thus, scaled PCP is especially appropriate for monitoring short-term drought.

Scaled LST has higher correlation with PDSI, PMDI, and Z-index than SPIs because PDSI, PMDI, and Z-index are based on the supply-and-demand concept, which are calculated from precipitation, temperature and available water capacity (AWC) of the soil (Palmer, 1965), while SPIs are calculated only from precipitation data (McKee et al., 1993).

Among all scaled variables, scaled SM shows the highest correlation with PDSI, PMDI, 6-month SPI, 9-month SPI, and 12-month SPI (Table 3). As the time scale of SPI increases from 1 to 9 months, the correlation coefficient increases, which indicates that soil moisture responds slowly to precipitation variations. The high correlation between scaled SM and PDSI/PMDI suggests that scaled SM is especially appropriate for agricultural drought monitoring, since PDSI and its variation, PMDI, were considered to be useful primarily for agricultural drought and other water uses that are sensitive to soil moisture (Guttman, 1998).

Generally, scaled NDVI (VCI) is not closely correlated with in-situ drought indices as other scaled variables (Table 3), because in-situ drought indices are mainly calculated from precipitation and temperature data and less directly convey vegetation information, while scaled NDVI reveals more information about drought influences on photosynthetic capacity of vegetation canopy, greenness level, leaf area index, and biomass. Among all in-situ drought indices, scaled NDVI shows higher correlation with PMDI, PDSI, and SPI of longer time scale (i.e., 3-month, 6-month, 9-month, and 12-month). The correlation coefficient increases as the time scale of SPI increases from 1-month to 12-month, an expected finding because of the lag of vegetation response to precipitation deficit.

We used PDSI to demonstrate the spatial variation of the correlations between scaled variables and in-situ drought indices (Fig. 2) because PDSI is very suitable for agricultural drought monitoring. The correlation coefficients between PDSI and scaled SM are higher than other scaled variables. With respect to the spatial variation, the scaled PCP, scaled LST, and scaled SM do not show any significant spatial patterns with PDSI over precipitation gradients. By contrast, an obvious spatial pattern exists for scaled NDVI (VCI) – correlation values with PDSI are higher in drier areas and lower in wetter areas (Fig. 2) because vegetation is more susceptible to drought variability in drier areas.

Overall, scaled SM provides valuable information for drought monitoring in addition to SDCI (combination of scaled NDVI, scaled LST, and scaled PCP) proposed by Rhee et al. (2010).

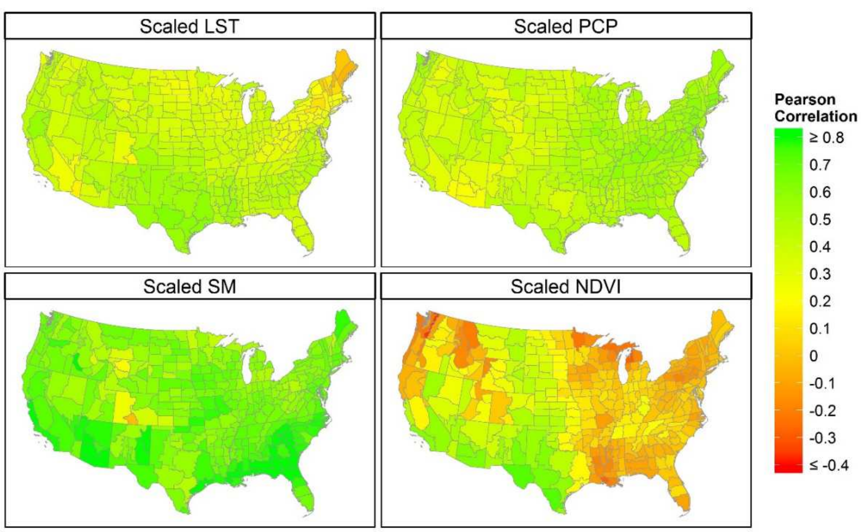

Fig. 2. Spatial variation of Pearson correlation coefficients between PDSI and scaled land surface temperature (LST), scaled precipitation (PCP), scaled soil moisture (SM), and scaled NDVI

4.2. Optimal Integrated Scaled Drought Index (ISDI)

We tested 15 systematic sets of weights to find and derive an optimal Integrated Scaled Drought Index (ISDI) (Table 4). Correlation analyses were performed between monthly in-situ drought indices and ISDI with different sets of weights. The highest three correlation coefficients for each in-situ drought index (each column) were highlighted (Table 4). The correlation coefficients are all statistically significant over 342 climate divisions between different in-situ drought indices and ISDIs (p-value < 0.01). Weight set 3 shows a particularly high correlation with the Z-index and 1-, 2-, and 3-month SPI values. Weight set 4 shows especially higher correlation with PDSI, PMDI and 6-, 9-, and 12-month SPI values. Weight set 9 shows higher correlation with PDSI, PMDI, and both shorter and longer time scale SPI (i.e., 2-month, 3-month, 6-month, 9-month, and 12-month). It shows the highest correlation with PDSI and 3-month SPI among all weights. PDSI and 3- and 6-month SPI are especially suitable for monitoring agricultural drought (Rouault & Richard, 2003). Thus, the linear combination of scaled LST, scaled PCP, scaled SM, and scaled NDVI with the weight set 9 (LST=1/6, PCP=1/3, SM=1/3, and NDVI=1/6) is selected as the optimal Integrated Scaled Drought Index (ISDI).

We compared the performance of ISDI with VHI (Table 4). ISDI shows much higher correlation with in-situ drought indices than VHI. We also compare the performance of ISDI with SDCI. Originally, SDCI uses MODIS and TRMM data, and here we alternatively used AVHRR and NARR data. Except for Z-index and 1-month SPI, ISDI shows higher correlation with in-situ drought indices (e.g., PDSI, PMDI, 2-month SPI, 3-month SPI, 6-month SPI, 9-month SPI, and 12-month SPI) than SDCI. Thus, ISDI generally performs better than both VHI and SDCI to correlate with in-situ drought indices.

Table 4 Averaged correlation coefficients between ISDI with 15 sets of weights and in-situ drought indices over 342 climate divisions. The highest three correlation coefficients for each in-situ drought index (each column) and the highest three sets of weights are shown in bold.

	Weights				Correlation coefficients								
NUM	Scaled LST	Scaled PCP	Scaled SM	Scaled NDVI	Z-index	PDSI	PMDI	SPI1	SPI2	SPI3	SPI6	SPI9	SPI12
1	1/4	1/4	1/4	1/4	0.697	**0.692**	0.714	0.589	0.628	0.637	0.620	0.597	0.568
2	2/5	1/5	1/5	1/5	0.642	0.641	0.659	0.509	0.558	0.572	0.561	0.533	0.504
3	**1/5**	**2/5**	**1/5**	**1/5**	**0.809**	0.679	0.689	**0.742**	**0.698**	**0.671**	0.603	0.562	0.527
4	**1/5**	**1/5**	**2/5**	**1/5**	0.633	**0.720**	**0.754**	0.516	0.604	0.637	**0.662**	**0.657**	**0.629**
5	1/5	1/5	1/5	2/5	0.614	0.633	0.656	0.510	0.569	0.586	0.568	0.557	0.535
6	1/3	1/3	1/6	1/6	**0.760**	0.658	0.668	**0.663**	0.644	0.628	0.575	0.531	0.497
7	1/3	1/6	1/3	1/6	0.614	0.688	0.717	0.477	0.565	0.597	0.620	0.606	0.578
8	1/3	1/6	1/6	1/3	0.597	0.616	0.635	0.467	0.532	0.552	0.540	0.521	0.497
9	**1/6**	**1/3**	**1/3**	**1/6**	0.748	**0.720**	**0.743**	0.664	**0.678**	**0.678**	**0.655**	**0.632**	**0.599**
10	1/6	1/3	1/6	1/3	**0.751**	0.650	0.662	**0.683**	**0.661**	0.643	0.578	0.546	0.517
11	1/6	1/6	1/3	1/3	0.587	0.688	0.722	0.473	0.573	0.611	0.633	**0.634**	**0.612**
12	2/7	2/7	2/7	1/7	0.723	0.702	0.723	0.615	0.641	0.646	0.628	0.600	0.567
13	2/7	2/7	1/7	2/7	0.724	0.643	0.655	0.627	0.624	0.614	0.562	0.527	0.497
14	2/7	1/7	2/7	2/7	0.584	0.671	0.702	0.449	0.548	0.585	0.605	0.598	0.574
15	1/7	2/7	2/7	2/7	0.711	0.702	0.726	0.626	0.655	0.661	0.639	0.622	0.593
VHI	1/2	0	0	1/2	0.308	0.368	0.380	0.161	0.263	0.299	0.303	0.292	0.283
SDCI	1/4	1/2	0	1/4	0.833	0.558	0.547	0.798	0.670	0.603	0.472	0.407	0.372

4.3. Validation using crop yield data

Corn is most sensitive to drought during the early reproductive stage (tasseling, silking, and pollination) (William L Kranz, Irmak, Van Donk, Yonts, & Martin, 2008). Droughts that occur during silking period can cause poor pollination and result in the greatest yields reduction (Berglund, Endres, & McWilliams, 2010; William L Kranz et al., 2008). Soybeans are most sensitive to drought during the mid- to late-reproductive stages: pod development and seed fill stages (Doss, Pearson, & Rogers, 1974; William L. Kranz & Specht, 2012). Droughts that occur during those periods can have the greatest impact on soybean yields potential, resulting in reduced number of seeds per pod and reduced seed size (William L. Kranz & Specht, 2012).

We performed correlation analyses between ISDI values during growing seasons (March to October) and corn/soybean yield anomalies from 1981 to 2013 for validation of the potential use of ISDI. Corn yield anomalies are higher correlated with ISDI in June, July, and August than other months, with the highest correlation in July. This period corresponds most closely with the early reproductive stage (tasseling/silking) for corn in most states, which is the most critical month for corn growth. Soybean yield anomalies are closely correlated with ISDI in July, August, and September than other months, with the highest correlation in August. This period corresponds to the critical mid- to late-reproductive stages of soybean: pod development and seed fill stages. Drought can significantly influence corn and soybeans during these critical growing periods as shown by the significant linear correlation between ISDI and corn (Fig. 3) and soybean (Fig. 4) yield anomalies (all p-values<0.001) for the 12 states with the highest annual corn/soybean production from 1981 to 2013. We excluded the outlier points in 1993 in Figure 3 and Figure 4 for Illinois, Iowa, Kansas, Minnesota, Missouri, Nebraska, North Dakota, South Dakota, and Wisconsin because from May to September of 1993, a major flooding occurred across those states along the Mississippi and Missouri rivers and their tributaries which severely impacted the agricultural production (Boruff, 1994; Johnson, Holmes, & Waite, 2004) and the lower-than-normal yields were caused by the flooding and excessive wetness instead of droughts. In addition, we selected four representative drought years: 1983, 1988, 2002, and 2012 to compare the spatial pattern of July/August ISDI and county-level corn/soybean yield anomalies, respectively. The county-level corn/soybean anomalies are calculated following the method of Lu et al. (2017). We find a very strong correspondence between July/August low ISDI values and lower-than-normal corn/soybean yield during those representative drought years (Fig. 5). These results partially illustrate the effectiveness and robustness of this new agriculturally-based drought index.

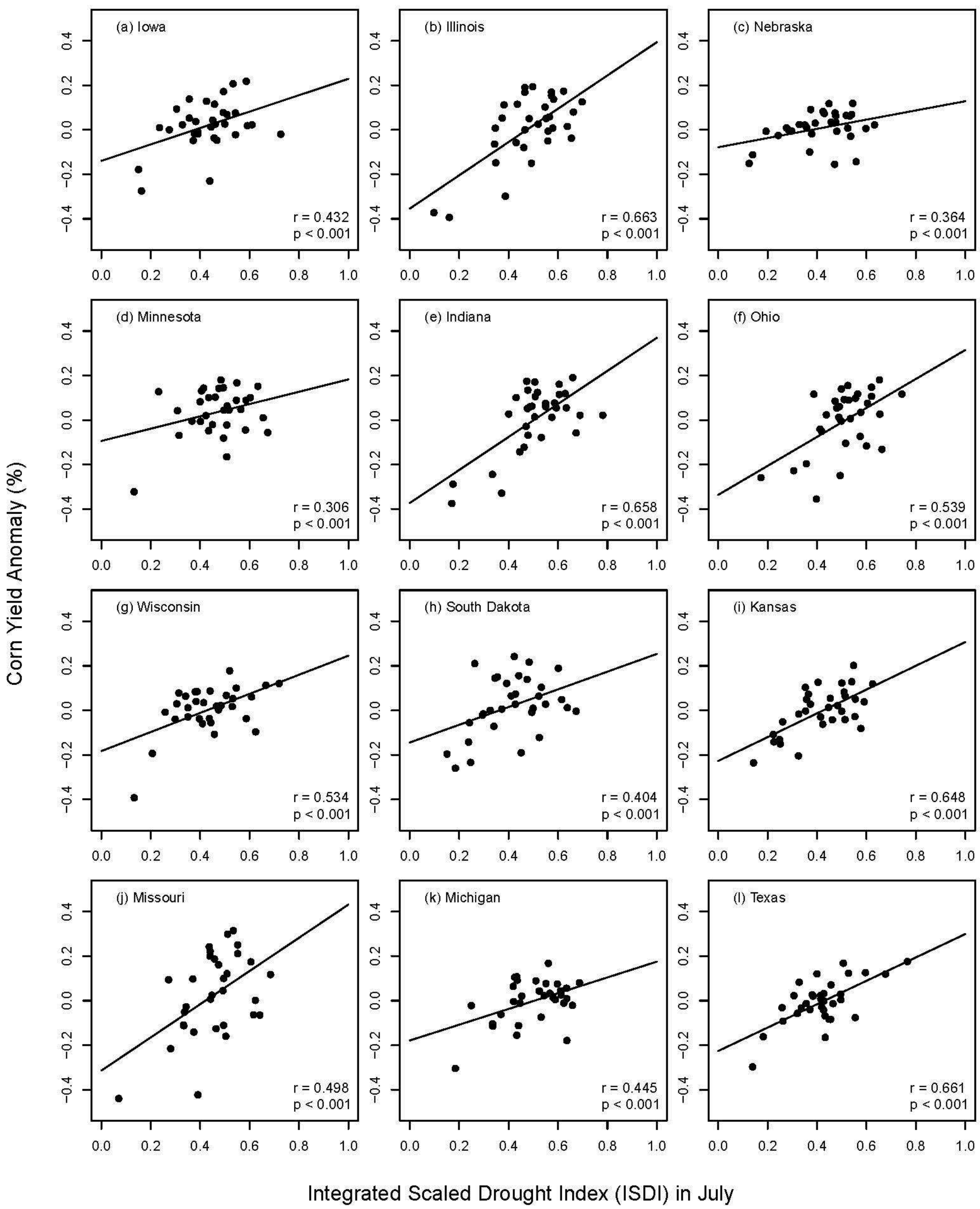

Fig. 3. Scatterplots and correlations between corn yield anomalies and the Integrated Scaled Drought Index (ISDI) in July for the 12 states with the highest annual corn production from 1981 to 2013 among all states: (a) Iowa, (b) Illinois, (c) Nebraska, (d) Minnesota, (e) Indiana, (f) Ohio, (g) Wisconsin, (h) South Dakota, (i) Kansas, (j) Missouri, (k) Michigan, and (l) Texas in the US

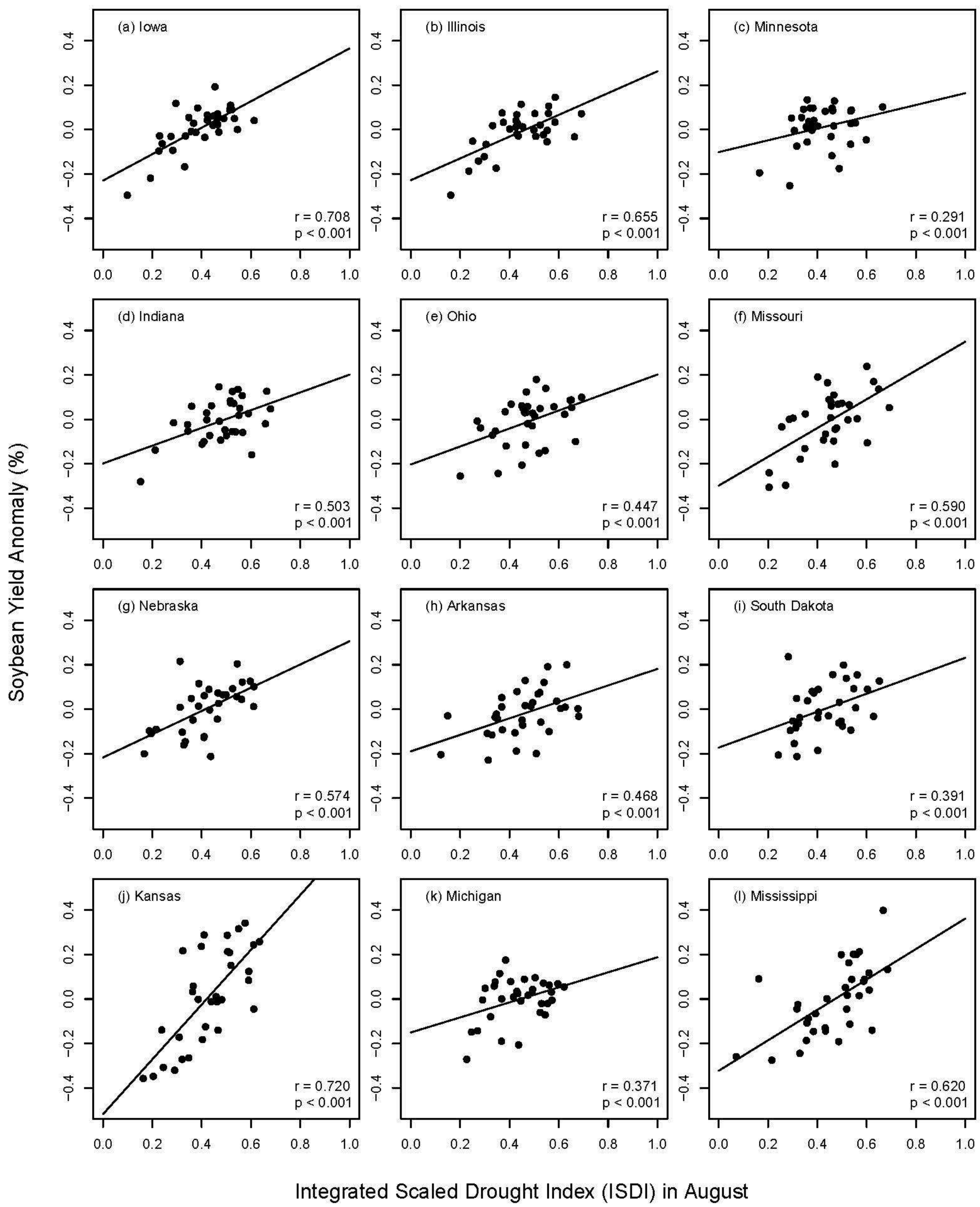

Fig. 4. Scatterplots and correlations between soybean yield anomalies and the Integrated Scaled Drought Index (ISDI) in August for the 12 states with the highest annual soybean production from 1981 to 2013 among all states: (a) Iowa, (b) Illinois, (c) Minnesota, (d) Indiana, (e) Ohio, (f) Missouri, (g) Nebraska, (h) Arkansas, (i) South Dakota, (j) Kansas, (k) Michigan, and (l) Mississippi in the US

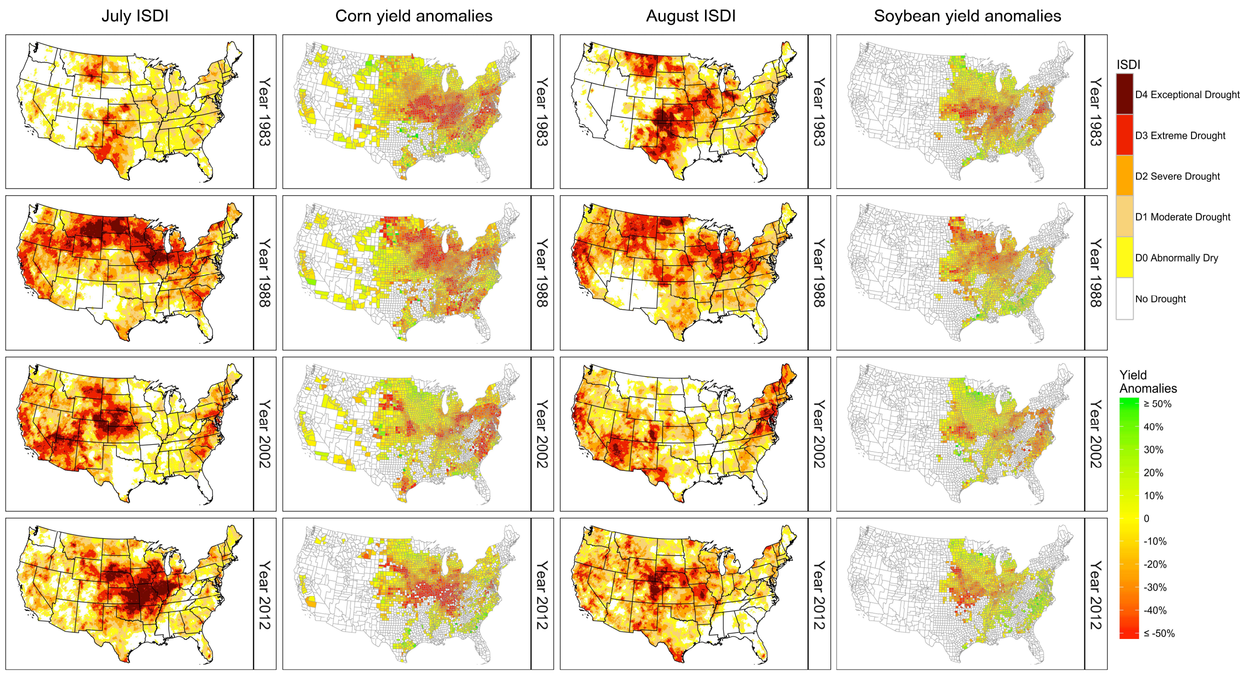

Fig. 5. Spatial pattern of July/August Integrated Scaled Drought Index (ISDI) and corn/soybean yield anomalies in 1983, 1988, 2002, and 2012 in the US (the first column: July ISDI; the second column: corn yield anomalies; the third column: August ISDI; the fourth column: soybean yield anomalies).

4.4. Empirical comparison with USDM maps and VegDRI maps

ISDI shows the highest correlation with corn and soybean yield anomalies in July and August, respectively, the two months most critical for corn and soybean growth. USDM maps are available from 2000 to present and VegDRI maps are available from 2009 to present. So, we choose to do a year-to-year comparison between ISDI and USDM maps in July from 2000 to 2013 and a year-to-year comparison between ISDI and VegDRI maps in August from 2009 to 2013 for empirical validation of ISDI. Also, we used gridded 3-month SPI maps calculated from PRISM data as an in-situ drought reference, since the time scale of 3-month is considered very appropriate for agricultural drought monitoring (Rouault & Richard, 2003).

Generally, the annual changes and spatial distribution of ISDI agree well with USDM maps in July from 2000 to 2013. The ISDI could provide much more detailed information when compared with USDM (Fig. 6). USDM is not a strictly quantitative product but the state-of-the-art blend of science and subjectivity including experts input (Svoboda et al., 2002), while ISDI is a completely quantitative product without expert inputs. The ISDI does not agree with USDM in earlier years (i.e., 2000 and 2001), but agrees very well in later years (Fig. 6). In 2000, ISDI detected a more severe drought west of the 100° W meridian and in the south of Texas than USDM did. In 2001, ISDI also detected a more severe drought in the south of Texas than the USDM did. Generally, ISDI shows better agreement with 3-month SPI calculated from PRISM than USDM in most years (Fig. 6).

Overall, ISDI agrees quite well with VegDRI maps to show US drought conditions in August from 2009 to 2013 (Fig. 7). In 2009, ISDI and VegDRI both detected extreme and severe droughts in the coastal Northwest, the West, and the Southwest, and extreme drought in south Texas. In 2010, they both detected scattered drought conditions. In 2011, they both detected severe and extreme drought conditions in the South. In 2012, they both showed severe and extreme droughts across the entire United States. In 2013, they both detected drought condition in the Northwest, West, Southwest, and South. However, ISDI detected severe drought in the Upper Midwest and Ohio Valley, but VegDRI did not. The severe drought conditions shown in those areas from the 3-month SPI indicates the better performance of ISDI in 2013 (Fig. 7). These comparisons with USDM maps, VegDRI maps, and gridded 3-month SPI maps illustrate the effectiveness and robustness of ISDI.

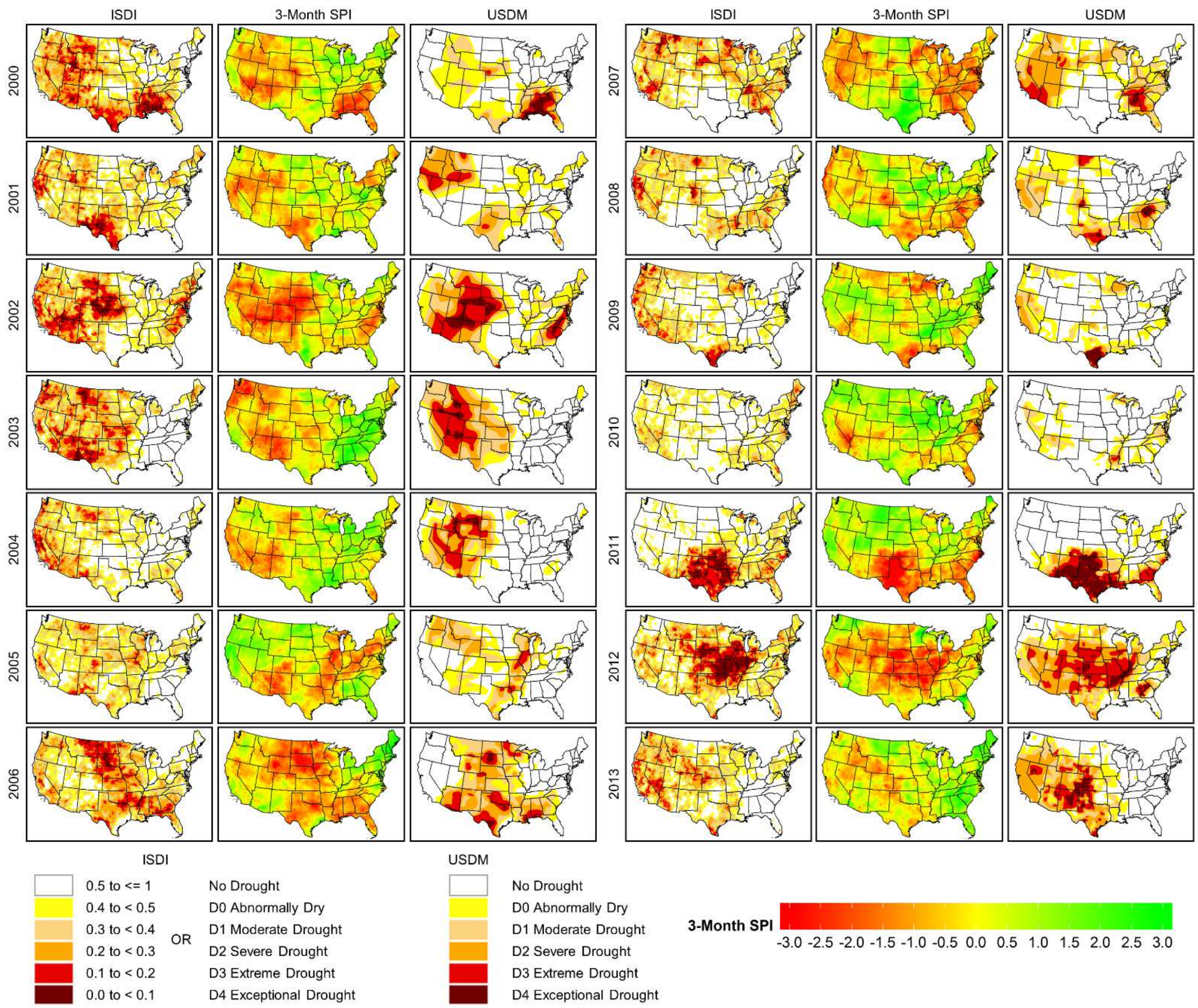

Fig. 6. Comparisons between Integrated Scaled Drought Index (ISDI), gridded 3-month SPI from prism data, and the United States Drought Monitor (USDM) maps in July from 2000 to 2013.

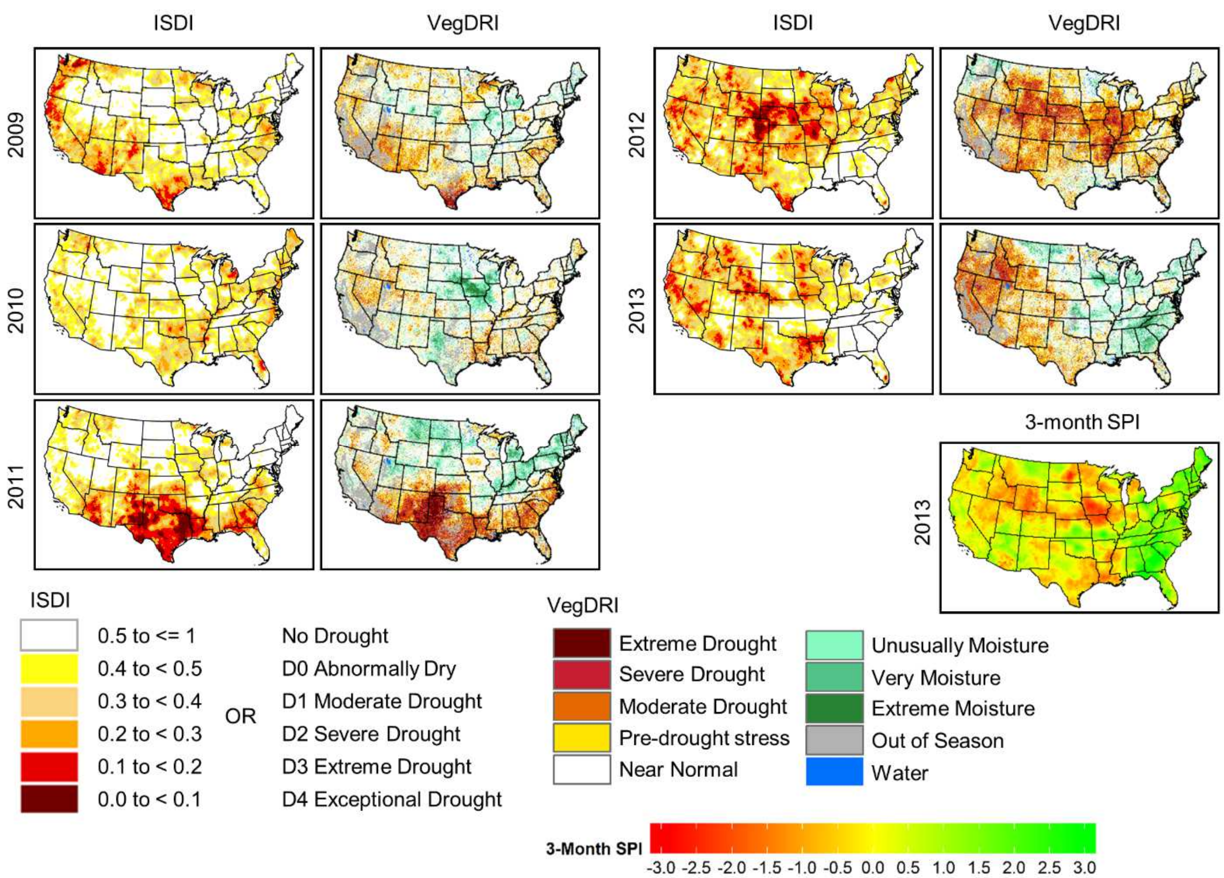

Fig. 7. Comparisons between Integrated Scaled Drought Index (ISDI) and the Vegetation Drought Response Index (VegDRI) maps in August from 2009 to 2013.

5. Conclusion

This study successfully develops a new monthly agriculturally-based drought index, the Integrated Scaled Drought Index (ISDI) which integrates four components (scaled NDVI, scaled land surface temperature (LST), scaled precipitation (PCP), and scaled soil moisture (SM)) to account for interannual variability of drought during the longest possible time-frame of the satellite era. We used long-term satellite-based observations of vegetation conditions from GIMMS AVHRR NDVI (available from 1981 to present) and climate conditions from NECP North American Regional Reanalysis (NARR) data (available from 1979 to present) to calculate the ISDI from 1981 to 2013 to make the long-term agricultural drought quantifications and measurements possible. Our results provide a long-term climatology of drought monitoring over the US which is beneficial for historical drought impacts assessment and future drought monitoring.

This new drought index incorporates a range of important variables controlling agricultural drought process, especially as it integrates soil moisture, an important but infrequently observed in-situ variable. Among all scaled variables, scaled soil moisture shows the highest correlation with PDSI, PMDI, and SPI at longer time scales (i.e., 6-month, 9-month, and 12-month), which suggests that scaled soil moisture can provide valuable information to monitor agricultural drought. Among the four components in this new drought index, we highlight the significance of the soil moisture component in agricultural drought monitoring. The ISDI with optimum weights shows much higher correlations with in-situ drought indices than VHI. Except for the Z-index and 1-month SPI, ISDI shows higher correlation with in-situ drought indices (i.e., PDSI, PMDI, 2-month SPI, 3-month SPI, 6-month SPI, 9-month SPI, and 12-month SPI) than SDCI. The ISDI performs better than VHI and SDCI to correlate with in-situ drought indices.

This new monthly drought index measures agricultural drought in the long-term and over large regions in a consistent and quantitative fashion. This index adds a new tool to the current toolbox of available methods to monitor and assess agricultural drought conditions on a monthly time step. The results indicate that the ISDI can identify historical major drought events and show potential for future operational implementation in drought monitoring and assessment. ISDI shows highest correlations with corn yield anomalies in July, which corresponds to the early reproductive stage (tasseling/silking) of corn, and shows highest correlation with soybean yield anomalies in August, which corresponds to the pod development and seed fill stages of soybean, periods when corn and soybean are most sensitive to water stress. There are significant linear correlations between ISDI and state-level corn and soybean yield anomalies. Additionally, a very strong spatial correspondence can be found between July/August low ISDI values and lower-than-normal corn/soybean yield during the four representative drought years (i.e., 1983, 1988, 2002, and 2012). Further, ISDI agrees very well with the two national-wide drought monitoring systems: USDM and VegDRI maps, and can detect year-to-year changes of drought conditions in the US. The above results all indicate a good performance of ISDI to monitor agricultural drought. This index can be generalized to incorporate other satellite data, numerical model simulations, or in-situ observations to monitor the agricultural drought, such as soil moisture data from Soil Moisture Active Passive (SMAP), precipitation data from Tropical Rainfall Measuring Mission (TRMM) or other precipitation radar data, temperature data from AVHRR and MODIS, NDVI data from MODIS, etc.

Reference:

AMS. (1997). Meteorological drought — Policy statement. *Bulletin of the American Meteorological Society, 78*, 847-849.

AMS. (2013). Drought — An Information Statement of the American Meteorological Society. Retrieved from https://www.ametsoc.org/ams/index.cfm/about-ams/ams-statements/statements-of-the-ams-in-force/drought/

Becker, E. J., Berbery, E. H., & Higgins, R. W. (2009). Understanding the Characteristics of Daily Precipitation over the United States Using the North American Regional Reanalysis. *Journal of Climate, 22*(23), 6268-6286. doi:10.1175/2009JCLI2838.1

Berglund, D. R., Endres, G. J., & McWilliams, D. A. (2010). *Corn growth and management quick guide*. Retrieved from https://www.ag.ndsu.edu/pubs/plantsci/crops/a1173.pdf

Boruff, C. S. (1994). Impacts of the 1993 Flood on Midwest Agriculture. *Water International, 19*(4), 212-215. doi:10.1080/02508069408686233

Brown, J. F., Wardlow, B. D., Tadesse, T., Hayes, M. J., & Reed, B. C. (2008). The Vegetation Drought Response Index (VegDRI): A New Integrated Approach for Monitoring Drought Stress in Vegetation. *GIScience & Remote Sensing, 45*(1), 16-46. doi:10.2747/1548-1603.45.1.16

Choi, W., Kim, S. J., Rasmussen, P. F., & Moore, A. R. (2009). Use of the North American Regional Reanalysis for Hydrological Modelling in Manitoba. *Canadian Water Resources Journal / Revue canadienne des ressources hydriques, 34*(1), 17-36. doi:10.4296/cwrj3401017

Daly, C., Halbleib, M., Smith, J. I., Gibson, W. P., Doggett, M. K., Taylor, G. H., . . . Pasteris, P. P. (2008). Physiographically sensitive mapping of climatological temperature and precipitation across the conterminous United States. *International Journal of Climatology, 28*(15), 2031-2064. doi:10.1002/joc.1688

Doss, B. D., Pearson, R. W., & Rogers, H. T. (1974). Effect of Soil Water Stress at Various Growth Stages on Soybean Yield1. *Agronomy Journal, 66*(2), 297-299. doi:10.2134/agronj1974.00021962006600020032x

Gao, B. (1996). NDWI—A normalized difference water index for remote sensing of vegetation liquid water from space. *Remote Sensing of Environment, 58*(3), 257-266. doi:10.1016/S0034-4257(96)00067-3

Gao, P., Carbone, G. J., & Guo, D. (2016). Assessment of NARCCAP model in simulating rainfall extremes using a spatially constrained regionalization method. *International Journal of Climatology, 36*(5), 2368-2378. doi:10.1002/joc.4500

Gu, Y., Brown, J. F., Verdin, J. P., & Wardlow, B. (2007). A five-year analysis of MODIS NDVI and NDWI for grassland drought assessment over the central Great Plains of the United States. *Geophysical Research Letters, 34*(6), L06407. doi:10.1029/2006GL029127

Guttman, N. B. (1998). Comparing the Palmer Drought Index and the Standardized Precipitation Index. *Journal of the American Water Resources Association, 34*(1), 113-121. doi:10.1111/j.1752-1688.1998.tb05964.x

Heddinghaus, T. R., & Sabol, P. (1991). *A review of the Palmer Drought Severity Index and where do we go from here*. Paper presented at the Proceedings of the seventh conference on applied climatology.

Heim, R. R. (2002). A review of twentieth-century drought indices used in the United States. *Bulletin of the American Meteorological Society, 83*(8), 1149-1165. doi:10.1175/1520-0477-83.8.1149

Homer, C., Dewitz, J., Fry, J., Coan, M., Hossain, N., Larson, C., . . . Wickham, J. (2007). Completion of the 2001 National Land Cover Database for the conterminous United States. *Photogrammetric engineering and remote sensing, 73*(4), 337-341.

IPCC. (2001). *Climate Change 2001: Impacts, Adaptation, and Vulnerability. Contribution of Working Group II to the Third Assessment Report of the Intergovernmental Panel on Climate Change* (J. J. McCarthy, O. F. Canziani, N. A. Leary, D. J. Dokken, & K. S. White Eds.). Cambridge, United Kingdom and New York, NY, USA: Cambridge University Press.

Johnson, G. P., Holmes, R. R., & Waite, L. A. (2004). *The great flood of 1993 on the upper mississippi river: 10 years later*. Retrieved from http://il.water.usgs.gov/pubs/fs2004-3024.pdf

Karnauskas, K. B., Ruiz-Barradas, A., Nigam, S., & Busalacchi, A. J. (2008). North American Droughts in ERA-40 Global and NCEP North American Regional Reanalyses: A Palmer Drought Severity Index Perspective. *Journal of Climate, 21*(10), 2102-2123. doi:10.1175/2007JCLI1837.1

Keyantash, J., & Dracup, J. A. (2002). The quantification of drought: An evaluation of drought indices. *Bulletin of the American Meteorological Society, 83*(8), 1167-1180. doi:10.1175/1520-0477-83.8.1167

Kogan, F. N. (1995a). Droughts of the Late 1980s in the United States as Derived from NOAA Polar-Orbiting Satellite Data. *Bulletin of the American Meteorological Society, 76*(5), 655-668. doi:10.1175/1520-0477(1995)076<0655:DOTLIT>2.0.CO;2

Kogan, F. N. (1995b). Application of vegetation index and rightness temperature for drought detection. *Advances in Space Research*, *15*(11), 91-100. doi:10.1016/0273-1177(95)00079-T

Kranz, W. L., Irmak, S., Van Donk, S. J., Yonts, C. D., & Martin, D. L. (2008). *Irrigation management for corn (NebGuide G1850)*. Retrieved from http://extensionpublications.unl.edu/assets/pdf/g1850.pdf

Kranz, W. L., & Specht, J. E. (2012). *Irrigating soybean (NebGuide G1367)*. Retrieved from http://extensionpublications.unl.edu/assets/pdf/g1367.pdf

Leeper, R. D., Bell, J. E., Vines, C., & Palecki, M. (2016). An Evaluation of the North American Regional Reanalysis Simulated Soil Moisture Conditions during the 2011 to 2013 Drought Period. *Journal of Hydrometeorology, 18*(2), 515-527. doi:10.1175/jhm-d-16-0132.1

Lu, J., Carbone, G. J., & Gao, P. (2017). Detrending crop yield data for spatial visualization of drought impacts in the United States, 1895–2014. *Agricultural and Forest Meteorology*, *237–238*, 196-208. doi:10.1016/j.agrformet.2017.02.001

McKee, T. B., Doesken, N. J., & Kleist, J. (1993). *The relationship of drought frequency and duration to time scales.* Paper presented at the Proceedings of the 8th Conference on Applied Climatology, American Meteorological Society Boston, MA.

Mesinger, F., DiMego, G., Kalnay, E., Mitchell, K., Shafran, P. C., Ebisuzaki, W., . . . Shi, W. (2006). North American Regional Reanalysis. *Bulletin of the American Meteorological Society*, *87*(3), 343-360. doi:10.1175/BAMS-87-3-343

Mishra, V., & Cherkauer, K. A. (2010). Retrospective droughts in the crop growing season: Implications to corn and soybean yield in the Midwestern United States. *Agricultural and Forest Meteorology*, *150*(7-8), 1030-1045. doi:10.1016/j.agrformet.2010.04.002

Mo, K. C., & Chelliah, M. (2006). The Modified Palmer Drought Severity Index Based on the NCEP North American Regional Reanalysis. *Journal of Applied Meteorology and Climatology*, *45*(10), 1362-1375. doi:10.1175/JAM2402.1

NOAA. (2018). NOAA National Centers for Environmental Information (NCEI) U.S. Billion-Dollar Weather and Climate Disasters. Retrieved from https://www.ncdc.noaa.gov/billions/

Palmer, W. C. (1965). *Meteorological drought* (Vol. Research Paper No. 45). Washington, DC, USA: U.S. Weather Bureau, U.S. Department of Commerce.

Peters, A. J., Walter-Shea, E. A., Ji, L., Vina, A., Hayes, M., & Svoboda, M. D. (2002). Drought monitoring with NDVI-based standardized vegetation index. *Photogrammetric engineering and remote sensing, 68*(1), 71-75.

Pinzon, J. E., & Tucker, C. J. (2014). A Non-Stationary 1981–2012 AVHRR NDVI3g Time Series. *6*(8), 6929.

Quiring, S. M., & Papakryiakou, T. N. (2003). An evaluation of agricultural drought indices for the Canadian prairies. *Agricultural and Forest Meteorology, 118*(1-2), 49-62. doi:10.1016/S0168-1923(03)00072-8

Rhee, J., Im, J., & Carbone, G. J. (2010). Monitoring agricultural drought for arid and humid regions using multi-sensor remote sensing data. *Remote Sensing of Environment, 114*(12), 2875-2887. doi:10.1016/j.rse.2010.07.005

Rouault, M., & Richard, Y. (2003). Intensity and spatial extension of drought in South Africa at different time scales. *water SA, 29*(4), 489-500. doi:10.4314/wsa.v29i4.5057

Rouse, J. W., Jr., Haas, R. H., Schell, J. A., & Deering, D. W. (1974). Monitoring vegetation systems in the Great Plains with ERTS. *NASA special publication, 351*, 309.

Ruiz-Barradas, A., & Nigam, S. (2006). Great Plains Hydroclimate Variability: The View from North American Regional Reanalysis. *Journal of Climate, 19*(12), 3004-3010. doi:10.1175/JCLI3768.1

Shafer, B. A., & Dezman, L. E. (1982). *Development of a Surface Water Supply Index (SWSI) to assess the severity of drought conditions in snowpack runoff areas.* Paper presented at the Proceedings of the Western Snow Conference.

Sheffield, J., Goteti, G., Wen, F., & Wood, E. F. (2004). A simulated soil moisture based drought analysis for the United States. *Journal of Geophysical Research: Atmospheres, 109*(D24), 1-19. doi:10.1029/2004JD005182

Svoboda, M., LeComte, D., Hayes, M., Heim, R., Gleason, K., Angel, J., . . . Stephens, S. (2002). The Drought Monitor. *Bulletin of the American Meteorological Society, 83*(8), 1181-1190. doi:10.1175/1520-0477(2002)083<1181:TDM>2.3.CO;2

Trnka, M., Hlavinka, P., Semeradova, D., Dubrovsky, M., Zalud, Z., & Mozny, M. (2007). Agricultural drought and spring barley yields in the Czech Republic. *Plant Soil and Environment, 53*(7), 306-316. doi:10.17221/2210-PSE

Tucker, C. J. (1979). Red and photographic infrared linear combinations for monitoring vegetation. *Remote Sensing of Environment, 8*(2), 127-150. doi:10.1016/0034-4257(79)90013-0

USDA. (2009). National crop progress - terms and definitions. Retrieved from http://www.nass.usda.gov/Publications/National_Crop_Progress/Terms_and_Definitions/

USDA. (2017). *United States Department of Agriculture - National Agricultural Statistics Service Database Quick Stats*. Retrieved from: https://quickstats.nass.usda.gov/

Vicente-Serrano, S. M., Beguería, S., & López-Moreno, J. I. (2010). A Multiscalar Drought Index Sensitive to Global Warming: The Standardized Precipitation Evapotranspiration Index. *Journal of Climate, 23*(7), 1696-1718. doi:10.1175/2009jcli2909.1

Vivoni, E. R., Tai, K., & Gochis, D. J. (2009). Effects of Initial Soil Moisture on Rainfall Generation and Subsequent Hydrologic Response during the North American Monsoon. *Journal of Hydrometeorology, 10*(3), 644-664. doi:10.1175/2008JHM1069.1

Wang, L. L., & Qu, J. J. (2007). NMDI: A normalized multi-band drought index for monitoring soil and vegetation moisture with satellite remote sensing. *Geophysical Research Letters, 34*(20). doi:10.1029/2007gl031021

Wickham, J. D., Stehman, S. V., Fry, J. A., Smith, J. H., & Homer, C. G. (2010). Thematic accuracy of the NLCD 2001 land cover for the conterminous United States. *Remote Sensing of Environment, 114*(6), 1286-1296. doi:10.1016/j.rse.2010.01.018

Wickham, J. D., Stehman, S. V., Gass, L., Dewitz, J. A., Sorenson, D. G., Granneman, B. J., . . . Baer, L. A. (2017). Thematic accuracy assessment of the 2011 National Land Cover Database (NLCD). *Remote Sensing of Environment, 191*, 328-341. doi:10.1016/j.rse.2016.12.026

Wilhite, D. A. (2000). Drought as a Natural Hazard: Concepts and Definitions. In D. A. Wilhite (Ed.), *Drought: A Global Assessment* (pp. 3-18). Routledge, London.

WMO. (1975). *Drought and Agriculture. WMO Technical Note 138*. Retrieved from https://library.wmo.int/opac/doc_num.php?explnum_id=1063